



# Extreme pressure conditions of BaS based materials: Detailed study of structural changes, band gap engineering, elastic constants and mechanical properties

Dejan Zagorac<sup>1,2,\*</sup>, Jelena Zagorac<sup>1,2</sup>, Klaus Doll<sup>3</sup>, Maria Čebela<sup>1,2</sup>, Branko Matović<sup>1,2</sup>

<sup>1</sup>*Institute of Nuclear Sciences Vinca, Materials Science Laboratory, Belgrade University, Belgrade, Serbia*

<sup>2</sup>*Center for synthesis, processing and characterization of materials for application in the extreme conditions, Belgrade, Serbia*

<sup>3</sup>*Institute of Theoretical Chemistry, University of Stuttgart, Stuttgart, Germany*

Received 5 July 2019; Received in revised form 1 November 2019; Accepted 21 November 2019

## Abstract

A Density Functional Theory (DFT) study has been performed in order to investigate behaviour of barium sulfide (BaS) at high pressures, and relationship between computed properties, in great detail. Novel predicted and previously synthesized BaS modifications have been calculated using Local Density Approximations (LDA) and Generalized Gradient Approximation (GGA) functionals. In particular, a detailed investigation of structural changes and its corresponding volume effect up to 100 GPa, with gradual pressure increase, has been performed from the first principles. Band gap engineering of the experimentally observed BaS phases at high pressures has been simulated and structure-property relationship is investigated. For each of the predicted and experimentally observed BaS structures, elastic constants and mechanical properties under compression have been investigated (e.g. ductility/brittleness, hardness, anisotropy). This study offers a new perspective of barium sulphide as a high pressure material with application in ceramics, optical and electrical technologies.

**Keywords:** DFT, mechanical properties, semiconductors, high pressure, barium sulphide

## I. Introduction

In the recent years, barium chalcogenides based materials have attracted great scientific and industrial interest due to their potential technological applications e.g. in microelectronics and magneto-optical devices [1–10]. Furthermore, due to their strong ionic character and metallization behaviour under high pressures [11,12] these compounds are promising candidates for various electrical and optical devices in the future [13,14]. Barium sulphide (BaS) is, like other barium chalcogenides, a wide-band gap semiconductor [15,16] with a large variety of applications. Although it is commonly used as a precursor to other Ba compounds, it is widely used in electronics, optics, paints and as an additive [14].

Under normal conditions BaS crystallizes in the rock-salt (NaCl) type of structure (Fig. 1a) [17–21]. In experimental and theoretical studies, a high pressure phase

transition from the NaCl to the cesium chloride (CsCl) type of structure was observed at pressures above 6 GPa (Fig. 1b) [17], similar to other chalcogenides [12–14,17–22]. Recently, a TII phase (Fig. 1c) has been suggested to occur along the NaCl → CsCl phase transition, as well as the possibility of the existence of a 5-5 and NiAs type of structure in the BaS system [23]. In addition, it has been reported that the cesium chloride phase starts to show a metallic character at pressures above 80 GPa [11,24].

There has been extensive theoretical work published on barium sulphide in the literature, mostly because of opto-electrical applications of barium chalcogenides. Most of these researches are focusing on the phase transitions, band structure, density of states (DOS), thermodynamic and elastic properties of well-known NaCl and CsCl modifications at standard conditions [25–32]. Here, the complete study of the structural, electronic and mechanical properties of barium sulphide has been presented, including experimentally observed modifications, as well as predicted (not-yet synthesized) BaS

\*Corresponding author: tel: +381 11 340 8545,  
e-mail: [dzagorac@vinca.rs](mailto:dzagorac@vinca.rs)

phases and their behaviour in the high pressure regime calculated with high precision DFT functionals.

## II. Computational methods

First principles calculations were performed using the modern CRYSTAL17 code [33] based on the linear combination of atomic orbitals (LCAO). The initial structure models used in this study were found in our previous searches of barium sulphide [23]. Full structural optimizations employed analytical gradients with respect to the atoms [34], cell parameters [35], and a local optimizing routine [36]. In our previous studies [23,37], we have found that Density Functional Theory (DFT) is an appropriate method for further investigation of BaS properties. In particular, a local density approximation (LDA) with the correlation functional by Perdew and Zunger (PZ) [38], and the Generalized Gradient Approximation (GGA) with the PBE (Perdew, Burke and Ernzerhof) functional [39] were used in this study. Fock/Kohn-Sham matrix mixing of 50% has been used in order to stabilize the total energy value of the calculated structures [40]. Tolerances for the convergence on total energy are set to  $1.0 \times 10^{-7} E_h$  per atom in each structural, electronic, elastic and mechanical properties calculations. A  $k$ -point mesh of size  $8 \times 8 \times 8$  in a Monkhorst-Pack scheme has been used.

An important part of the ab initio calculations is the basis set information and in BaS it plays a vital role in the properties calculations. Thus, a  $[5s4p1d]$  all-electron basis set was used for sulphur according to literature data [41–43]. In the case of barium, we have used the pseudopotential by Hay and Wadt [44] and in total a  $[4s4p2d]$  basis set as in our previous work [23,37], which contains a diffuse  $d$ -function. The diffuse  $d$ -function on Ba is crucial to obtain the proper conduction band structure and band gap of BaS [45–50]. Structure analysis and visualization were performed using the KPLOT [51] and the VESTA [52] program, while for visualization of Young's modulus anisotropy an open-

source application ELATE [53] has been used. A fully automated procedure to calculate second-order elastic constants (SOEC) has been used as implemented in the CRYSTAL17 code [54]. The bulk modulus is obtained from the compliance matrix elements, and other elastic properties such as shear modulus, Young's modulus, Poisson's ratio and quantities derived from the Voigt-Reuss-Hill approximation are obtained from the computed data [55]. The full elastic tensor has been generated by using the keyword ELASTCON. In order to obtain the elastic constants at a given pressure, we have performed a series of elastic calculations at the volume corresponding to the desired pressures,  $V(P)$ , using the recently developed module in the CRYSTAL code [56].

## III. Results and discussion

### 3.1. Structural changes of BaS at high pressure

The structural behaviour of barium sulphide with the increase of pressure has been investigated in great detail. At zero pressure conditions, BaS appears in the rock-salt (B1) type structure (Fig. 1a), while at high pressures it transforms to the CsCl type (B2, Fig. 1c). Both BaS modifications were optimized using first principles calculations with LDA and GGA, and the results were in a very good agreement with previous experimental [17–22,24] and theoretical results [11,12,23,25–30,47,48]. Since it has been observed that the calculated values of the cell parameters were slightly underestimated compared to the experimental values, while the GGA-PBE functional slightly overestimates (see supporting information, Table S1), each of the investigated properties in this study were calculated with both LDA and GGA approaches for comparison.

According to the experimental observations, the rock-salt structure transforms into a CsCl type modification with the increase of pressure above 6 GPa, where the two phases coexist above or below the transition pressure during the pressure increase or release, respec-

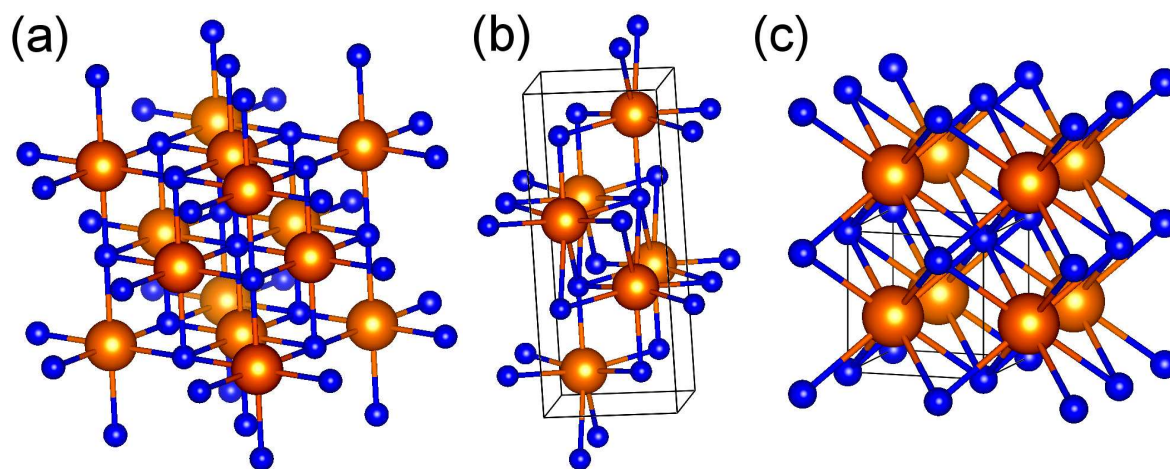


**Figure 1.** Visualization of the calculated structure types in barium sulphide: a) NaCl type, experimentally observed at standard conditions, b) TII type, predicted at high pressures and c) CsCl type, observed at high pressures (small (blue) and large (orange) spheres correspond to S and Ba atoms, respectively)

tively [17,24]. Again, our calculations were in a good agreement with the experimental data, since the B1 → B2 phase transition is found at 5.7 GPa using the LDA functional and 5.9 GPa using the GGA method. We note that no intermediate BaS phase has been experimentally observed during the B1 → B2 pressure induced phase transition. In the recent study, the TII (B33) modification (Fig. 1b) has been found as metastable structure very close to the transition region [23]. This type of phase transition (NaCl (B1) → TII (B33) → CsCl (B2)) is known to exist in TII [57,58] and PbS [42,48,59–63].

**Table 1. Unit cell parameters and corresponding volumes of the NaCl modification in the BaS compound under compression up to 10 GPa (calculations performed using LDA-PZ and GGA-PBE functionals)**

Pressure [GPa]	Cell parameters [Å]			Volume [Å <sup>3</sup> ]	
	Exp.	LDA	GGA	LDA	GGA
0	6.39 <sup>a</sup>	6.31	6.44	251.77	267.09
1	-	6.28	6.40	247.12	262.14
2	-	6.24	6.36	243.00	257.26
3	-	6.21	6.33	239.24	253.64
4	-	6.18	6.29	235.72	248.86
5	6.16 <sup>a</sup>	6.15	6.26	232.61	245.31
6	-	6.12	6.23	229.40	241.80
7	-	6.10	6.20	226.98	238.33
8	-	6.07	6.17	223.76	234.86
9	-	6.05	6.14	221.20	231.48
10	-	6.03	6.12	218.72	229.22

<sup>a</sup>experiment [17]

The structural behaviour of the rock-salt (B1) modification of BaS and its corresponding volume effect at high pressures has been investigated from the first principles. In particular, the NaCl modification has been submitted to constant increase of pressure of ~1 GPa (up to 10 GPa) using LDA and GGA methods (Table 1). As expected, the cell parameters and volumes monotonously decrease with increasing pressure regardless of the computational approach. We would like to note that the only experimental data for NaCl phase at high pressures available so far are measurements at 5 GPa, where our DFT calculations show good agreement. In order to further investigate the structural properties of barium sulphide at high pressure, the CsCl (B2) modification has been investigated on the DFT level. In particular, the CsCl modification has been submitted to constant increase of pressure of ~5 GPa (up to 100 GPa) using LDA and GGA approach (Table 2). Again, the results obtained at high pressures (at 6 GPa) for CsCl were in a very good agreement with previous experimental data regardless of the calculation method. Since this is the first detailed study of structural changes of barium sulphide at high pressure regime, we hope that it will help future experimental and theoretical studies of BaS in the high pressure regime.

**Table 2. Calculated unit cell parameters and corresponding volumes of the CsCl modification in the BaS compound at elevated pressures up to 100 GPa (calculations performed using LDA-PZ and GGA-PBE functionals)**

Pressure [GPa]	Cell parameters [Å]			Volume [Å <sup>3</sup> ]	
	Exp.	LDA	GGA	LDA	GGA
0	-	3.77	3.87	53.49	57.96
5	-	3.67	3.74	49.43	52.31
6	3.69 <sup>a</sup>	3.66	3.72	49.03	51.48
10	-	3.61	3.66	47.05	49.03
15	-	3.56	3.61	45.12	47.05
20	-	3.51	3.56	43.24	45.12
25	-	3.47	3.52	41.78	43.61
30	-	3.44	3.49	40.71	42.51
35	-	3.41	3.45	39.65	41.06
40	-	3.38	3.42	38.61	40.00
45	-	3.36	3.40	37.93	39.65
50	-	3.33	3.37	37.00	38.27
55	-	3.31	3.35	36.26	37.60
60	-	3.29	3.32	35.61	36.59
65	-	3.27	3.30	34.96	35.94
70	-	3.25	3.28	34.24	35.29
75	-	3.23	3.26	33.70	34.65
80	-	3.21	3.24	33.08	34.01
85	-	3.19	3.22	32.46	33.39
90	-	3.17	3.20	31.86	32.77
95	-	3.15	3.19	31.26	32.46
100	-	3.13	3.17	30.66	31.86

<sup>a</sup>experiment [17]

#### IV. BaS band gap engineering as function of pressure

In the second part of the study, a detailed investigation of electronic properties as a function of pressure has been performed. The experimentally observed modifications exhibiting the NaCl structure and the high pressure CsCl phase were optimized using the first principles calculations on LDA and GGA level. Their band structures, in particular band gap as function of pressure, were investigated. We note that our DFT results show very good agreement with available experimental data and can be used for high pressure investigations of BaS with high accuracy. There is some controversy in the literature, reporting barium sulphide as a direct band gap semiconductor with band gap of ~3.9 eV located at the  $\Gamma$ -point [15,16,64]. On the other hand, previous theoretical studies of the rock-salt phase in the BaS system have shown an indirect band gap (along the  $\Gamma \rightarrow X$  direction) ranging from 1.83 to 3.54 eV [26,45–50]. Our band structure calculations for equilibrium NaCl structure are shown in Fig. 2a, exhibiting a band gap size of 2.02 on LDA and 2.44 eV on GGA level. An indirect band gap along the  $\Gamma \rightarrow X$  direction of the Brillouin zone has been found regardless of the computational ap-

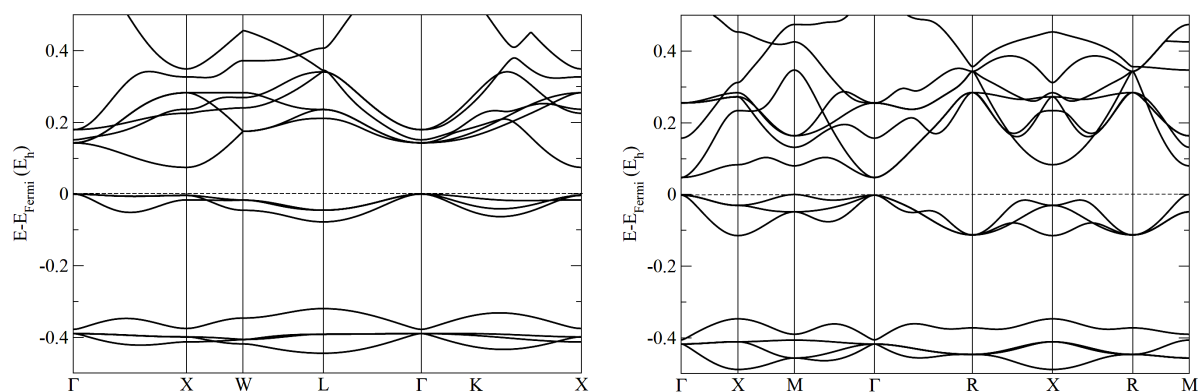


**Figure 2.** Band structure calculation performed using DFT-LDA of: a) the NaCl (B1) modification and b) the CsCl (B2) structure (note that the labels of the special points in the NaCl modification correspond to a face-centred cubic (*fcc*) lattice, while in the CsCl phase they correspond to the primitive (simple) cubic (*cP*) lattice, respectively)

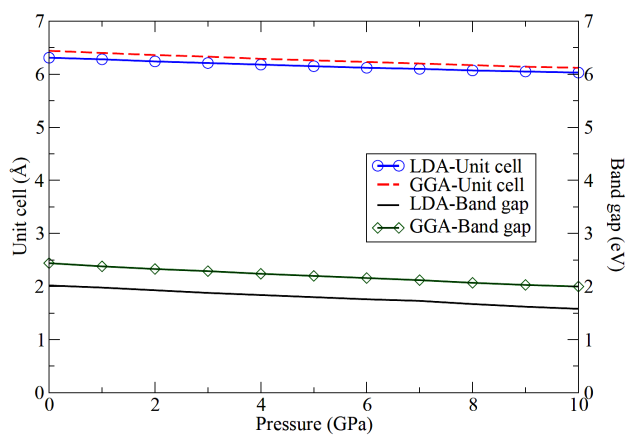


**Figure 3.** Calculated band gap of the NaCl modification in the BaS compound at elevated pressures up to 10 GPa (calculations performed using LDA-PZ and GGA-PBE functional)

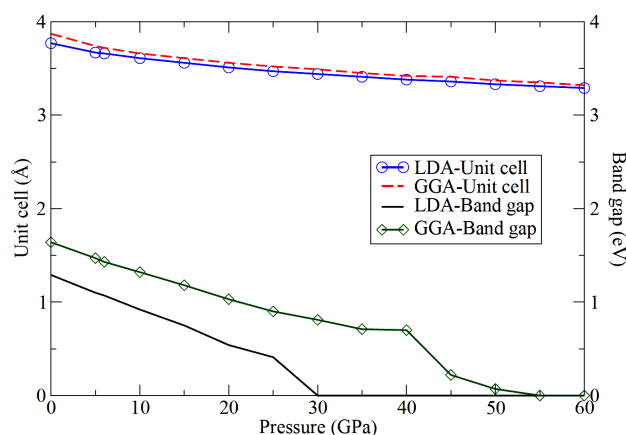
proach, which is again in a good agreement with literature data [23,26,45–50].

Figure 2b shows the band structure calculation of the CsCl modification in barium sulphide. The band gap of the CsCl modification has been calculated to 1.29 eV using LDA method and 1.64 eV using GGA-PBE. Again, an indirect band gap along the  $M \rightarrow \Gamma$  direction of the Brillouin zone has been observed regardless of the calculation method. The large shrinking of the CsCl band gap compared to the band gap of the rock-salt modification was of particular interest and its connection to the structural properties and the B1  $\rightarrow$  B2 phase transition at high pressures. Scarce literature data show that with the increase of pressure above 80 GPa CsCl phase becomes metallic [11,12,24]. However, in previous theoretical study involving DFT-LDA approximation, a metallization pressure of 32 GPa has been calculated [50]. Since there is a large spreading of theoretical and experimental data, and since there are no similar studies in the literature, a detailed investigation of the electronic properties of the CsCl and NaCl structure at high pressures has been performed.

The band gap of the rock-salt (B1) modification in BaS system has been calculated for a constant increase

of pressure of  $\sim 1$  GPa (up to 10 GPa) using LDA and GGA (Fig. 3 and Table S2 in supporting information). In general, the size of the band gap is found to be reduced with the increase of the pressure, regardless of the computational approach. In addition, a volume contraction with respect to changes in pressure and band gap size was analysed (Fig. 3 and Table S2). The decrease in unit cell size is connected with a decreasing gap, which clearly connects electronic and structural properties of barium sulphide.

Next, the electronic properties of the CsCl modification in the BaS system and the respective volume effect at calculated high pressures have been investigated on DFT level. In particular, the CsCl modification has been submitted to constant increase of pressure of  $\sim 5$  GPa (up to 60 GPa) using LDA and GGA (Fig. 4 and Table S3). Again, we observe a close connection of the structural and electronic properties of the CsCl structure in barium sulphide. The band gap decreases quickly at low-pressure conditions ( $<6$  GPa), followed by greater volume shrinkage (Fig. 4). Later, there is gradual decrease in band gap size up to 35 GPa at GGA, and up to 25 GPa with LDA level of theory. At 40 GPa the band gap is almost the same although the pressure is increased and



**Figure 4.** Calculated size of the band gap in the CsCl modification in the BaS compound at elevated pressures up to 60 GPa (calculations performed using LDA-PZ and GGA-PBE functional)

the unit cell and volume are decreased calculated with GGA, while the highest energy state of the valence band is hardly distinguishable between the M and the  $\Gamma$  point of the Brillouin zone (Fig. 5a).

Surprisingly, at 45 GPa the unit cell and the volume are hardly changed, however the band gap is further narrowed to 0.22 eV. Here, we would like to highlight another important result of this study. Figure 5b shows a CsCl phase calculated at 45 GPa using GGA approach. One can observe that at 45 GPa indirect band gap becomes a direct band gap at the  $\Gamma$  point, which might be connected to minor cell parameter and volume changes (Table 2 and S3). Furthermore, our results are in good agreement with previous studies, where CsCl

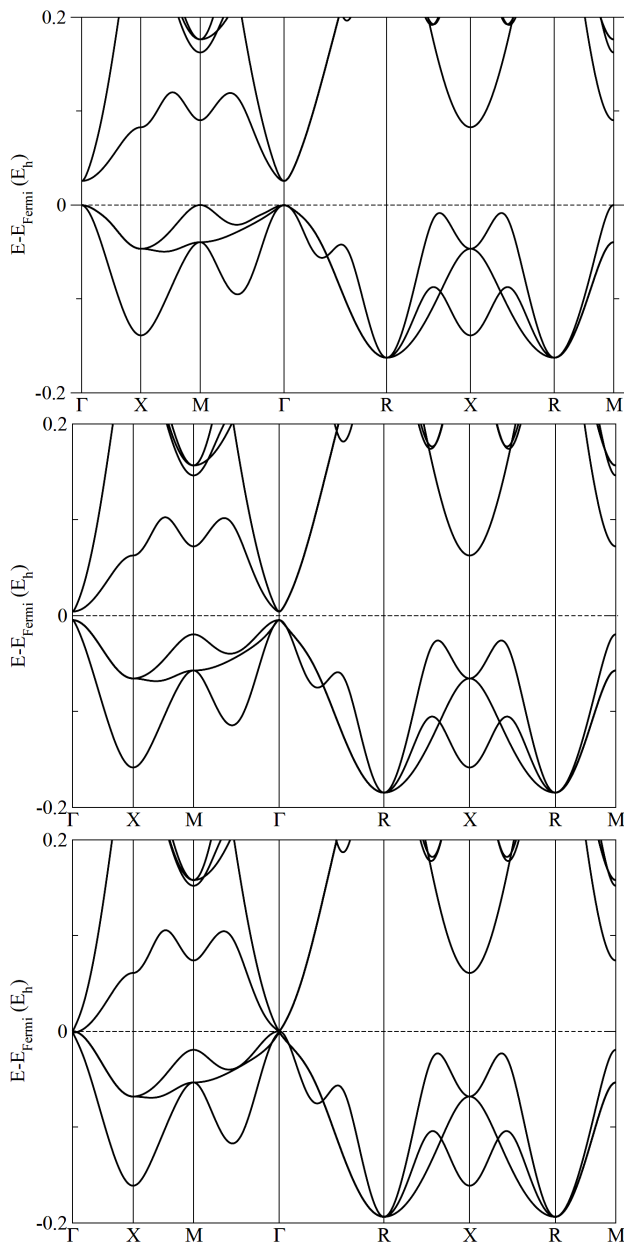


**Figure 5.** Band structure of the CsCl (B2) structure at: a) 40 GPa, b) 45 GPa showing direct band gap and c) 55 GPa exhibiting metallic properties (calculation performed using GGA-PBE)

has been shown to become a direct gap semiconductor with a transition at the  $\Gamma$  point in previous experimental and theoretical research of BaS at high pressures [11,23,24]. At 55 GPa, closing of the direct band gap has been observed, and CsCl modification becomes metallic at GGA-PBE level of theory (Fig. 5c). Furthermore, a calculation using the LDA functional shows metallic behaviour of the CsCl modification at pressures above 30 GPa, which is in very good agreement with previous theoretical studies [50].

In short, our detailed study showed a great diversity of the electronic properties of barium sulphide at high pressure regime. In principle, one could decrease the size of the band gap and influence the position of the gap, even changing the semiconducting-metallic character of BaS with the increase of pressure. Furthermore, direct bandgap materials tend to have stronger light emission and absorption properties, which in combination with indirect gap materials are used in photovoltaics (PVs), light emitting diodes (LEDs) and laser diodes. Thus, the band structure calculations show a close connection to the structural properties of BaS at high pressures, which can be used in industrial, scientific and/or technological applications to tune the electronic properties of barium sulphide.

## V. Mechanical properties of BaS at standard and elevated pressures

In the final part of this study we have investigated mechanical properties of the BaS compound at standard and high pressures. Figure 6 and Table S4 show a summary of calculated elastic coefficients of the most relevant BaS phases using the LDA functional (for GGA-PBE results see supporting information). Previous experimental and theoretical findings were collected, analysed and added to the following tables in order to compare the accuracy of the previous results with the present study. We observe that the calculated elastic constants for equilibrium rock-salt and high pressure CsCl modification presented in Fig. 6 and Tables S4 and S5 in

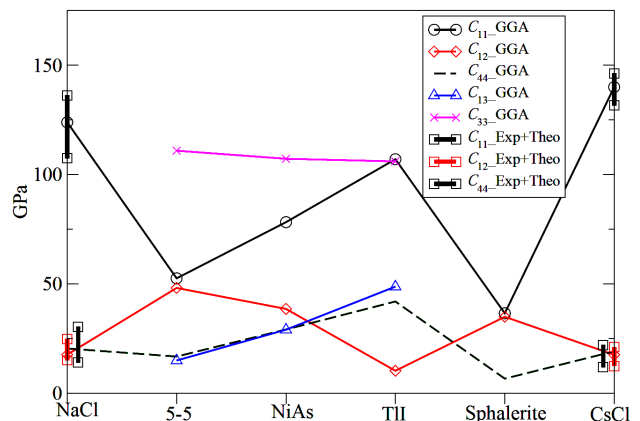


**Figure 6.** Calculated elastic coefficients of the most relevant barium sulphide modifications calculated using LDA functional

**Table 3. Bulk modulus  $B$ , shear modulus  $G$ , Pugh's delay/brittle criterion  $B/G$ , Young's modulus  $E$ , Young's modulus anisotropy factor  $A_y$ , Poisson's ratio  $\nu_h$  and hardness  $H_V$  calculated using GGA functional in BaS system**

Structure type	$B$ [GPa]	$G$ [GPa]	$B/G$	$E$ [GPa]	$A_y$	$\nu_h$	$H_V$ [GPa]
NaCl	44.8 (39.4–55.1) <sup>a,b</sup> (40.3–52.4) <sup>b-f</sup>	27.5	1.63	68.4	1.72	0.25	5.51
5-5	35.2	10.6	3.31	28.9	7.15	0.36	1.26
NiAs	42.7	23.8	1.79	60.3	1.64	0.26	4.48
TII	35.2	28.2	1.25	66.8	5.2	0.18	7.59
Sph	30.9	4.4	7.08	12.5	4.56	0.43	0.28
CsCl	47.9 (21.4–34.0) <sup>a,b</sup> (42.2–57.3) <sup>b-f</sup>	22.9	2.09	59.5	4.28	0.29	3.67

Previous works – <sup>a</sup> experiment [17], <sup>b</sup> experiment [24], <sup>c</sup> GGA, LDA [26], <sup>d</sup> GGA, LDA [65], <sup>e</sup> LDA [25] <sup>f</sup> LDA [66]

the supporting information are in good agreement with the great amount of previous theoretical work. Furthermore, when analysing previous results, one can observe great range of calculated elastic coefficients of barium sulphide modifications. However, our LDA calculations are in a good agreement with previous LDA and molecular dynamics (MD) studies [25,26,32,65,66], while GGA computations are in agreement with corresponding GGA theoretical reports from the literature [26,65].

Experimentally observed modifications of BaS, rock-salt, which appears at standard, and CsCl appearing at high pressures, together with a predicted sphalerite structure show cubic symmetry and they have only three independent elastic constants  $C_{11}$ ,  $C_{12}$  and  $C_{44}$  (Fig. 6). In further work, elastic constants were used to calculate other mechanical and elastic properties, such as the Poisson's ratio  $\nu$ , bulk modulus  $B$ , shear modulus  $G$ , and Young's modulus  $E$  [67]. The obtained values are given in Table 3 for six investigated barium sulphide structures. Again our results are in good agreement with previous studies for experimentally observed structures, while in the case of the predicted BaS phases this study is the first report of such properties.

Since the shear modulus  $G$  represents the resistance to plastic deformation, while the bulk modulus  $B$  represents the resistance to fracture, the relationship  $B/G$  has been calculated in order to link the mechanical properties of materials with its elastic modulus [68]. The critical value of Pugh's forecast material delay/brittle empirical criterion ( $B/G$ ) which separates ductile and brittle materials is around or higher than 1.75. If higher than this value, the material behaves in a ductile manner; otherwise, the material behaves in a brittle manner [69]. According to the ratio  $B/G$  given in Table 3 and Table S6 in the supporting information, each of the investigated BaS modifications is ductile regardless of calculation method applied, except for NaCl and TII structures which are computed as brittle using GGA. Furthermore, Poisson's ratio  $\nu$  also provides information about ductility/brittleness of the materials, and if the value of  $\nu$  is smaller than 0.26, the material will have brittle behaviour. It has been observed that the rock salt and the hexagonal structures have brittle behaviour, while others

are ductile according to Poisson's ratio calculated using GGA (see Table 3). On LDA level of theory all six investigated BaS modifications show ductile behaviour.

Young's modulus  $E$  is a very important constant for the mechanical properties of material. Small value of Young's modulus indicates better plasticity [70] and small values of Young's modulus for six BaS modifications are shown in Table 3 and Fig. 7. It has been found that the experimentally observed NaCl and CsCl modifications have the largest value of  $E$ , so the plasticity is the smallest compared to the other modifications. Since Young's modulus is also a measure of the stiffness of the solid, where higher value of  $E$  indicates higher stiffness, the corresponding BaS structures are also the stiffest. On the other hand, sphalerite modification has the largest plasticity, and the smallest stiffness among all other BaS modifications, which again can be attributed to the pressure changes.

The Vickers hardness  $H_V$  related to the elastic and plastic properties of polycrystalline materials [71] has been calculated and it is shown in Table 3. We note that the hardest modifications that could be synthesized are the high pressure phases, the TII modification at GGA level of calculation (Table 3), and CsCl modification using LDA (Table S6). A summary of all mechanical properties plotted for each of the investigated modifi-

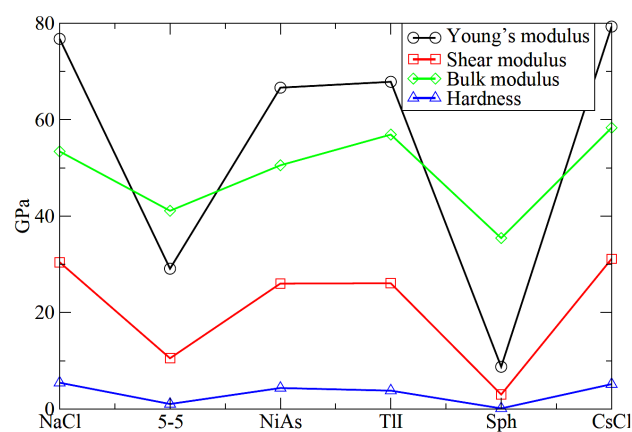


**Figure 7. Calculated Young's modulus  $E$ , shear modulus  $K$ , bulk modulus  $B$  and hardness  $H_V$  for BaS modifications on LDA level of theory**

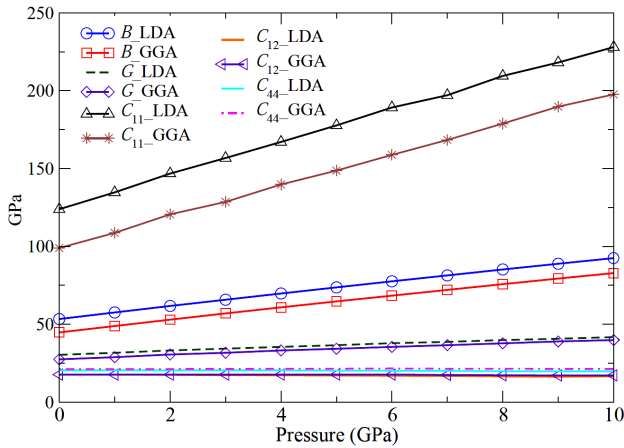


**Figure 8. Bulk modulus  $B$ , shear modulus  $G$  and elastic constants ( $C_{11}$ – $C_{44}$ ) as function of pressure in the rock-salt modification of BaS calculated using LDA and GGA**

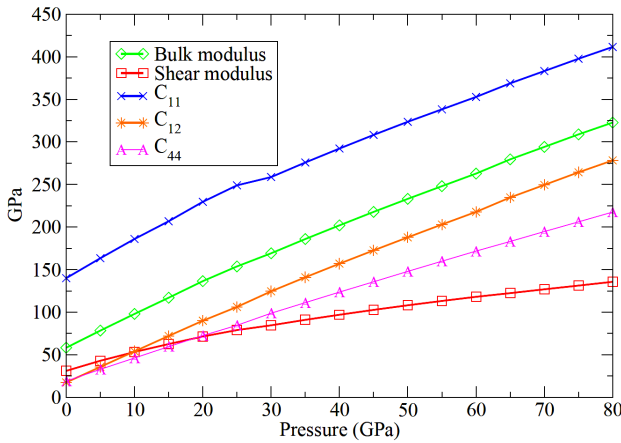


**Figure 9. High pressure behaviour of bulk modulus  $B$ , shear modulus  $G$  and elastic constants ( $C_{11}$ – $C_{44}$ ) in the CsCl modification of BaS calculated using LDA**

cations of barium sulphide is presented in Fig. 7. We observe that most of the mechanical properties have the highest values in the experimentally observed NaCl and CsCl modifications, while the lowest are appearing in the cubic sphalerite and hexagonal 5-5 modifications, regardless of computational approach applied. Interestingly, the high pressure TII structure and high temperature NiAs phase have similar mechanical properties.

The bulk modulus can also be described as the resistance to the volume change under pressure [67,71]. For cubic modifications, the bulk modulus mainly depends on the elastic constants  $C_{11}$  and  $C_{12}$  and since the elastic constant  $C_{12}$  is smaller than  $C_{11}$  for the calculated cubic modifications (NaCl, CsCl and ZnS), the constant  $C_{11}$  mainly determines the value of  $B$ . In hexagonal structures, the dominant influence on the bulk modulus is due to the  $C_{33}$  elastic constant. At standard pressures the highest values of bulk modulus are found in experimentally observed NaCl and CsCl modifications, which means that they have the best capacity of resistance to volume change under pressure. This has been investigated in great detail in the previous chapter, and we have

further investigated mechanical properties and elastic constants of NaCl and CsCl modifications at high pressures.

A summary of calculated bulk modulus, shear modulus and elastic constants ( $C_{11}$ – $C_{44}$ ) as function of pressure up to 10 GPa in the rock-salt modification in BaS system calculated using LDA and GGA is shown in Fig. 8 and Table S7. It has been observed that the calculated bulk and shear modulus gradually increase with the increase of pressure regardless of computational method. Similar effect has been observed in the  $C_{11}$  elastic constant, which was expected since its value mainly determines the value of  $B$ . However, for the elastic constants  $C_{12}$  and  $C_{44}$ , initially a small increase of the parameters and then a decrease with further increase of pressure is observed. This could be related to the pressure driven phase transition of barium sulphide.

Similarly, bulk modulus, shear modulus, and elastic constants ( $C_{11}$ – $C_{44}$ ) as function of pressure up to 80 GPa of the cesium chloride modification of BaS calculated using LDA and GGA have been investigated and a summary is shown in Fig. 9 and Table S8 of the supporting information (exact calculated values are presented in Table S8). It has been observed that the calculated bulk and shear modulus gradually increase with the increase of pressure regardless of computational approach (Fig. 9). In the CsCl structure, this trend was followed in all calculated elastic constants ( $C_{11}$ – $C_{44}$ ) on contrary to the rock salt modification of the BaS compound.

Finally, the elastic anisotropy, related to the material microcracks and nanoscale precursor textures, has been investigated. In order to illustrate the Young's modulus anisotropy  $A_y$  for the investigated BaS modifications (Table 3), the 3D anisotropic surface figures of Young's modulus under the spherical coordinates were plotted (Fig. 10). Since the content of anisotropy depends on the degree of deviation from the spherical shape, a great degree of elastic anisotropy has been observed. In particular, the smallest elastic anisotropy has been observed in the 5-5 and NiAs structures (Figs. 10b and 10c), while the largest elastic anisotropy has been found in the case of the TII and the ZnS modifications (Fig. 10d and 10e), compared to the experimentally observed barium sulphide phases.

## VI. Conclusions

A detailed study of the high pressure behaviour of structural changes, band gap engineering, elastic constants and mechanical properties of barium sulphide has been performed using Density Functional Theory (DFT). The local density approximation with the correlation functional by Perdew and Zunger, and the Generalized Gradient Approximation with the Perdew, Burke and Ernzerhof functional were used in this study. Our calculations show good agreement with previous experimental and theoretical results involving the equilibrium NaCl (B1) and high pressure CsCl (B2) phase. In particular, a detailed investigation of structural and elec-

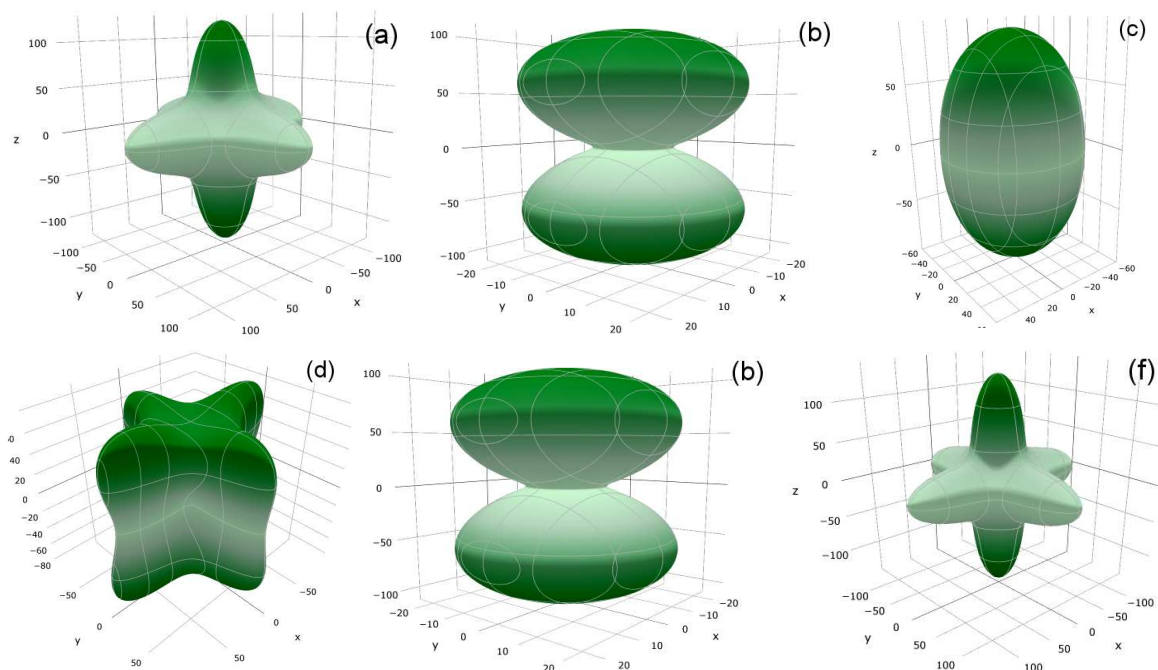


**Figure 10.** 3D contour plots of Young's modulus anisotropy for a) NaCl, b) 5-5, c) NiAs, d) TiI, e) sphalerite and f) CsCl modifications of BaS on LDA level of theory

tronic properties of the experimentally observed BaS phases at high pressures has been performed. In principle, one could decrease the size of the band gap, influence the position of the gap and even changing the semiconducting-metallic character of BaS with the increase of pressure. In addition, several barium sulphide structures have been predicted and calculated on *ab initio* level. Together with the experimentally observed BaS modifications, their mechanical and elastic properties have been investigated. Furthermore, ductility, brittleness, hardness, and calculated elastic constants at various pressures have been investigated, as well as the relationship between calculated hardness, Young's modulus, bulk modulus and shear modulus. This study offers a new perspective of barium sulphide as a high pressure material with various technological applications, e.g. photovoltaics (PVs), light emitting diodes (LEDs) and laser diodes.

**Acknowledgement:** The authors thank to prof. R. Dovesi and Crystal Solutions for software support. The authors thank Max Planck Institute for Solid State Research, Stuttgart, Germany, for collaboration and providing computational support. This work has been supported by the Ministry of Education, Science and Technological Development of the Republic of Serbia under the grant No. 45012.

§ Supporting information can be downloaded using following link: <https://bit.ly/2tVeda4>

## References

1. B. Khalfallah, F.-Z. Driss-Khodja, F. Saadaoui, M. Driss-Khodja, A. Boudali, H. Bendaoud, B. Bouhafis, "A first-principles study of the structural, elastic, electronic, vibrational, and optical properties of  $\text{BaSe}_{1-x}\text{Te}_x$ ", *J. Comput. Electron.*, **17** [4] (2018) 1478–1491.
2. S. Drablia, N. Boukhris, R. Boulechfar, H. Meradji, S. Ghemid, R. Ahmed, S. Bin Omran, F.E.H. Hassan, R. Khenata, "Ab initio calculations of the structural, electronic, thermodynamic and thermal properties of  $\text{BaSe}_{1-x}\text{Te}_x$  alloys", *Phys. Scripta*, **92** [10] (2017) 105701.
3. Z. Addadi, B. Doumi, A. Mokaddem, M. Elkeurti, A. Sayede, A. Tadjer, F. Dahmane, "Electronic and ferromagnetic properties of 3d(V)-doped (BaS) barium sulfide", *J. Superconduct. Novel Magn.*, **30** [4] (2017) 917–923.
4. S.G.E.T. Escher, T. Lazauskas, M.A. Zwijnenburg, S.M. Woodley, "Structure prediction of  $(\text{BaO})_n$  nanoclusters for  $n \leq 24$  using an evolutionary algorithm", *Comput. Theor. Chem.*, **1107** (2017) 74–81.
5. A.S. Patra, M.S. Chauhan, S. Keene, G. Gogoi, K.A. Reddy, S. Ardo, D.L.V.K. Prasad, M. Qureshi, "Combined experimental and theoretical insights into the synergistic effect of cerium doping and oxygen vacancies in  $\text{BaZrO}_{3-\delta}$  hollow nanospheres for efficient photocatalytic hydrogen production", *J. Phys. Chem. C*, **123** [1] (2019) 233–249.
6. Y. Han, S. Siol, Q. Zhang, A. Zakutayev, "Optoelectronic properties of strontium and barium copper sulfides prepared by combinatorial sputtering", *Chem. Mater.*, **29** [19] (2017) 8239–8248.
7. C.M. Schurz, T. Schleid, "Single crystals of the isotypic series  $\text{BaLu}_2\text{Ch}_4$  (Ch = S, Se and Te) with  $\text{CaFe}_2\text{O}_4$ -type structure", *Crystals*, **1** [3] (2011) 78–86.
8. T. Prikhna, M. Eisterer, H.W. Weber, W. Gawalek, X. Chaud, V. Sokolovsky, V. Moshchil, A. Kozyrev, V. Sverdun, R. Kuznietsov, T. Habisreuther, M. Karpets, V. Kovylaev, J. Noudem, J. Rabier, A. Joulain, W. Goldacker, T. Basyuk, V. Tkach, J. Dellith, C. Schmidt, A. Shaternik, "Pinning in  $\text{MgB}_2$ - and  $\text{YBaCuO}$ -based superconductors: Effect of manufacturing pressure and temperature", *IEEE Trans. Appl. Superconduct.*, **23** [3] (2013) 8001605.
9. E. Bittarello, M. Bruno, D. Aquilano, "Ab initio calcu-



- lations of the main crystal surfaces of baryte ( $\text{BaSO}_4$ )”, *Crystal Growth Design*, **18** [7] (2018) 4084–4094.
10. Y. Li, D.J. Singh, “Tunability of electronic and optical properties of the Ba-Zr-S system via dimensional reduction”, *Eur. Phys. J. B*, **91** [8] (2018) 188.
  11. P. Cervantes, Q. Williams, M. Côté, M. Rohlfing, M.L. Cohen, S.G. Louie, “Band structures of CsCl-structured BaS and CaSe at high pressure: Implications for metallization pressures of the alkaline earth chalcogenides”, *Phys. Rev. B*, **58** [15] (1998) 9793–9800.
  12. T.A. Grzybowski, A.L. Ruoff, “Band-overlap metallization of BaTe”, *Phys. Rev. Lett.*, **53** [5] (1984) 489–492.
  13. K.L. Heng, S.J. Chua, P. Wu, “Prediction of semiconductor material properties by the properties of their constituent chemical elements”, *Chem. Mater.*, **12** [6] (2000) 1648–1653.
  14. E. Wiberg, N. Wiberg, A.F. Holleman, *Inorganic Chemistry*, Academic Press, De Gruyter, San Diego, Berlin, New York, 2001.
  15. R.J. Zollweg, “Optical absorption and photoemission of barium and strontium oxides, sulfides, selenides, and tellurides”, *Phys. Rev.*, **111** [1] (1958) 113–119.
  16. Y. Kaneko, K. Morimoto, T. Koda, “Optical properties of alkaline-earth chalcogenides. II. Vacuum ultraviolet reflection spectra in the synchrotron radiation region of 4–40 eV”, *J. Phys. Soc. Jpn.*, **52** [12] (1983) 4385–4396.
  17. S. Yamaoka, O. Shimomura, H. Nakazawa, O. Fukunaga, “Pressure-induced phase transformation in BaS”, *Solid State Commun.*, **33** [1] (1980) 87–89.
  18. S. Holgersson, “Die Struktur der Sulfide von Mg, Ca, Sr und Ba”, *Z. Anorgan. Allg. Chem.*, **126** (1923) 179–182.
  19. T. Petzel, “Über die Darstellung von CaS, SrS und BaS aus den Metallen und Schwefelwasserstoff in flüssigem Ammoniak”, *Z. Anorgan. Allg. Chem.*, **396** (1973) 173–177.
  20. H.D.H. Rad, R. “Über Thiomercurate. 2. Zur Kenntnis von  $\text{Ba}_2\text{HgS}_3$ ”, *Z. Anorgan. Allg. Chem.*, **483** (1981) 7–17.
  21. O.J. Güntert, A. Faessler, “Präzisionsbestimmung der Gitterkonstanten der Erdalkalisulfide MgS, CaS, SrS und BaS”, *Z. Kristallograph.*, **107** (2010) 357–361.
  22. T.A. Grzybowski, A.L. Ruoff, “High-pressure phase transition in BaSe”, *Phys. Rev. B*, **27** [10] (1983) 6502–6503.
  23. D. Zagorac, K. Doll, J. Zagorac, D. Jordanov, B. Matović, “Barium sulfide under pressure: Discovery of metastable polymorphs and investigation of electronic properties on ab initio level”, *Inorgan. Chem.*, **56** [17] (2017) 10644–10654.
  24. S.T. Weir, Y.K. Vohra, A.L. Ruoff, “High-pressure phase transitions and the equations of state of BaS and BaO”, *Phys. Rev. B*, **33** [6] (1986) 4221–4226.
  25. E. Tuncel, K. Colakoglu, E. Deligoz, Y.O. Ciftci, “A first-principles study on the structural, elastic, vibrational, and thermodynamical properties of BaX (X = S, Se, and Te)”, *J. Phys. Chem. Solids*, **70** [2] (2009) 371–378.
  26. A. Bouhemadou, R. Khenata, F. Zegrar, M. Sahnoun, H. Baltache, A.H. Reshak, “Ab initio study of structural, electronic, elastic and high pressure properties of barium chalcogenides”, *Comput. Mater. Sci.*, **38** [2] (2006) 263–270.
  27. P.K. Jha, U.K. Sakalle, S.P. Sanyal, “High pressure structural phase transition in alkaline earth chalcogenides”, *J. Phys. Chem. Solids*, **59** [9] (1998) 1633–1637.
  28. M. Durandurdu, “Pressure-induced phase transformation of BaS: An ab initio constant pressure study”, *Chem. Phys.*, **367** [2] (2010) 80–82.
  29. O. Potzel, G. Taubmann, “The pressure induced B1-B2 phase transition of alkaline halides and alkaline earth chalcogenides. A first principles investigation”, *J. Solid State Chem.*, **184** [5] (2011) 1079–1084.
  30. M. Teng, X. Hong, “Phase transition and thermodynamic properties of BaS: An ab initio study”, *Wuhan Uni. J. Natural Sci.*, **16** [1] (2011) 33–37.
  31. X. Zhou, J.L. Roehl, C. Lind, S.V. Khare, “Study of B1 (NaCl-type) to B2 (CsCl-type) pressure-induced structural phase transition in BaS, BaSe and BaTe using ab initio computations”, *J. Phys.: Condens. Mat.*, **25** [7] (2013) 075401.
  32. J.P. Rino, “An interaction potential for barium sulfide: A molecular dynamics study”, *Comput. Mater. Sci.*, **92** (2014) 334–342.
  33. R. Dovesi, A. Erba, R. Orlando, C.M. Zicovich-Wilson, B. Civalleri, L. Maschio, M. Rérat, S. Casassa, J. Baima, S. Salustro, B. Kirtman, “Quantum-mechanical condensed matter simulations with CRYSTAL”, *Wiley Interdiscip. Rev.: Comput. Mol. Sci.*, **8** (4) (2018) e1360.
  34. K. Doll, V.R. Saunders, N.M. Harrison, “Analytical Hartree-Fock gradients for periodic systems”, *Int. J. Quantum Chem.*, **82** [1] (2001) 1–13.
  35. K. Doll, “Analytical stress tensor and pressure calculations with the CRYSTAL code”, *Mol. Phys.*, **108** [3-4] (2010) 223–227.
  36. B. Civalleri, P. D’Arco, R. Orlando, V.R. Saunders, R. Dovesi, “Hartree-Fock geometry optimisation of periodic systems with the Crystal code”, *Chem. Phys. Lett.*, **348** [1] (2001) 131–138.
  37. D. Zagorac, K. Doll, J.C. Schön, M. Jansen, “Sterically active electron pairs in lead sulfide? An investigation of the electronic and vibrational properties of PbS in the transition region between the rock salt and the  $\alpha$ -GeTe-type modifications”, *Chem. Eur. J.*, **18** (35) (2012) 10929–10936.
  38. J.P. Perdew, A. Zunger, “Self-interaction correction to density-functional approximations for many-electron systems”, *Phys. Rev. B*, **23** [10] (1981) 5048–5079.
  39. J.P. Perdew, K. Burke, M. Ernzerhof, “Generalized gradient approximation made simple”, *Phys. Rev. Lett.*, **77** [18] (1996) 3865–3868.
  40. R. Dovesi, R. Orlando, A. Erba, C.M. Zicovich-Wilson, B. Civalleri, S. Casassa, L. Maschio, M. Ferrabone, M. De La Pierre, P. D’Arco, Y. Noël, M. Causà, M. Rérat, B. Kirtman, “CRYSTAL14: A program for the ab initio investigation of crystalline solids”, *Int. J. Quantum Chem.*, **114** [19] (2014) 1287–1317.
  41. M. Mian, N.M. Harrison, V.R. Saunders, W.R. Flavell, “An ab initio Hartree-Fock investigation of galena (PbS)”, *Chem. Phys. Lett.*, **257** [5] (1996) 627–632.
  42. D. Zagorac, K. Doll, J.C. Schön, M. Jansen, “Ab initio structure prediction for lead sulfide at standard and elevated pressures”, *Phys. Rev. B*, **84** [4] (2011) 045206.
  43. D. Zagorac, J. Zagorac, J.C. Schön, N. Stojanovic, B. Matovic, “ZnO/ZnS (hetero)structures: ab initio investigations of polytypic behavior of mixed ZnO and ZnS compounds”, *Acta Cryst. B*, **74** [6] (2018) 628–644.
  44. P.J. Hay, W.R. Wadt, “Ab initio effective core potentials for molecular calculations. Potentials for K to Au including the outermost core orbitals”, *J. Chem. Phys.*, **82** [1] (1985) 299–310.

45. A. Pourghazi, M. Dadsetani, “Electronic and optical properties of BaTe, BaSe and BaS from first principles”, *Phys. B: Condens. Mat.*, **370** [1] (2005) 35–45.
46. K.C. Mishra, K.H. Johnson, P.C. Schmidt, “A comparative study of electronic structure of alkaline earth sulfides as hosts for phosphors”, *Mater. Sci. Eng. B*, **18** [3] (1993) 214–219.
47. G. Kalpana, B. Palanivel, M. Rajagopalan, “Electronic structure and structural phase stability in BaS, BaSe, and BaTe”, *Phys. Rev. B*, **50** [17] (1994) 12318–12325.
48. G.Q. Lin, H. Gong, P. Wu, “Electronic properties of barium chalcogenides from first-principles calculations: Tailoring wide-band-gap II-VI semiconductors”, *Phys. Rev. B*, **71** [8] (2005) 085203.
49. Z. Feng, H. Hu, Z. Lv, S. Cui, “First-principles study of electronic and optical properties of BaS, BaSe and BaTe”, *Central Eur. J. Phys.*, **8** [5] (2010) 782–788.
50. A.E. Carlsson, J.W. Wilkins, “Band-overlap metallization of BaS, BaSe, and BaTe”, *Phys. Rev. B*, **29** [10] (1984) 5836–5839.
51. R. Hundt, *KPLOT, A Program for Plotting and Analyzing Crystal Structures*, Technicum Scientific Publishing, Stuttgart, Germany, 2016.
52. K. Momma, F. Izumi, “VESTA: a three-dimensional visualization system for electronic and structural analysis”, *J. Appl. Crystallogr.*, **41** [3] (2008) 653–658.
53. G. Romain, P. Pluton, C. François-Xavier, “ELATE: an open-source online application for analysis and visualization of elastic tensors”, *J. Phys.: Condens. Mat.*, **28** (27) (2016) 275201.
54. W.F. Perger, J. Criswell, B. Civalleri, R. Dovesi, “Ab-initio calculation of elastic constants of crystalline systems with the CRYSTAL code”, *Computer Phys. Commun.*, **180** [10] (2009) 1753–1759.
55. J.F. Nye, *Physical Properties of Crystals*, Dover Publications, New York, 1957.
56. A. Erba, A. Mahmoud, D. Belmonte, R. Dovesi, “High pressure elastic properties of minerals from ab initio simulations: The case of pyrope, grossular and andradite silicate garnets”, *J. Chem. Phys.*, **140** [12] (2014) 124703.
57. A.-V. Mudring, “Thallium halides - New aspects of the stereochemical activity of electron lone pairs of heavier main-group elements”, *Eur. J. Inorg. Chem.*, **2007** [6] (2007) 882–890.
58. R.P. Lowndes, C.H. Perry, “Molecular structure and anharmonicity in thallium iodide”, *J. Chem. Phys.* **58** [1] (1973) 271–278.
59. D. Zagorac, K. Doll, J.C. Schön, M. Jansen, “Structure prediction for PbS and ZnO at different pressures and visualization of the energy landscapes”, *Acta Phys. Polonica A*, **120** (2011) 215–220.
60. T. Chattopadhyay, H.G. von Schnering, W.A. Grosshans, W.B. Holzapfel, “High pressure X-ray diffraction study on the structural phase transitions in PbS, PbSe and PbTe with synchrotron radiation”, *Physica B+C*, **139-140** (1986) 356–360.
61. G. Andrzej, F. Karen, “Pressure-induced orthorhombic structure of PbS”, *J. Phys.: Condens. Mat.*, **22** [9] (2010) 095402.
62. S. Wang, J. Zhang, Y. Zhang, A. Alvarado, J. Attapattu, D. He, L. Wang, C. Chen, Y. Zhao, “Phase-transition induced elastic softening and band gap transition in semiconducting PbS at high pressure”, *Inorg. Chem.*, **52** [15] (2013) 8638–8643.
63. D. Ferhat, B. Savas, “Ab initio investigation of B16(GeS), B27(FeB) and B33(CrB/TiI) phases of lead chalcogenides”, *Phys. Scripta*, **88** [1] (2013) 015603.
64. G.A. Saum, E.B. Hensley, “Fundamental optical absorption in the IIA-VIB compounds”, *Phys. Rev.*, **113** [4] (1959) 1019–1022.
65. F. El Haj Hassan, H. Akbarzadeh, “First-principles elastic and bonding properties of barium chalcogenides”, *Comput. Mater. Sci.*, **38** [2] (2006) 362–368.
66. A. Benamrani, K. Kassali, K. Bouamama, “Pseudopotential study of barium chalcogenides under hydrostatic pressure”, *High Pressure Res.*, **30** [1] (2010) 207–218.
67. M. Ashby, H. Shercliff, D. Cebon, *Materials, Engineering, Science, Processing and Design*, Elsevier: Butterworth-Heinemann, University of Cambridge, 2008.
68. S.F. Pugh, “XCII. Relations between the elastic moduli and the plastic properties of polycrystalline pure metals”, *Philos. Magaz. J. Sci.*, **45** [367] (1954) 823–843.
69. G. Vaitheeswaran, V. Kanchana, R.S. Kumar, A.L. Cornelius, M.F. Nicol, A. Svane, A. Delin, B. Johansson, “High-pressure structural, elastic, and electronic properties of the scintillator host material  $\text{KMgF}_3$ ”, *Phys. Rev. B*, **76** [1] (2007) 014107.
70. A. Sumer, J.F. Smith, “Elastic constants of single-crystal  $\text{CaMg}_2$ ”, *J. Appl. Phys.*, **33** [7] (1962) 2283–2286.
71. Y. Tian, B. Xu, Z. Zhao, “Microscopic theory of hardness and design of novel superhard crystals”, *Int. J. Refract. Met. Hard Mater.*, **33** (2012) 93–106.